Synthesis and luminescence of monohalogenated $B_{18}H_{22}$ clusters

Kierstyn P. Anderson,[a] Arnold L. Rheingold,[b] Peter I. Djurovich,[c] Ovie Soman,[a] Alexander M. Spokoyny[a]*

[a]*Department of Chemistry and Biochemistry and California NanoSystem Institute (CNSI), University of California, Los Angeles, California 90095, USA*

[b]*Department of Chemistry, University of California, San Diego, La Jolla, California 92093, USA*

[c]*Department of Chemistry, University of Southern California, Los Angeles, California 90089, USA*

***Corresponding Author Information**

E-mail: spokoyny@chem.ucla.edu

Abstract

This work advances the foundation of *anti*-$B_{18}H_{22}$ chemistry by exploring cluster reactivity in the context of monohalogenation and the luminescent properties of the resulting compounds. The synthesis and photoluminescent properties of new *anti*-$B_{18}H_{22}$ derivatives 4-I-$B_{18}H_{21}$ and 7-Cl-$B_{18}H_{21}$ are described and benchmarked against other existing monohalogenated species reported previously. Electrophilic halogenation utilizing $AlCl_3$ and I_2 produces iodination at the B4 vertex to produce 4-I-$B_{18}H_{21}$ in 43% isolated yield. This compound exhibits oxygen-insensitive phosphorescence at 514 nm (Φ = 0.16). Chlorination of the B7 vertex through treatment of the parent borane with N-chlorosuccinimide and hydrochloric acid gives 7-Cl-$B_{18}H_{21}$ in 76% isolated yield, which produces fluorescent emission at 418 nm and exhibits one of the highest quantum yields of $B_{18}H_{22}$ derivatives reported to date, Φ = 0.80.

1. Introduction

Among the molecular luminescent materials containing boron,[1] *anti*-$B_{18}H_{22}$ is the only inherently fluorescent unfunctionalized polyhedral boron hydride known to date, exhibiting a quantum yield of 0.97.[2] This compound has recently gained more widespread attention due to its promise for optoelectronic applications, such as lasers, OLEDs and UV-imaging.[3] Despite this, much is still unknown regarding the synthetic diversification routes for *anti*-$B_{18}H_{22}$ and how substitutions at the boron vertices can alter its luminescent profile. The synthetic chemistry of *anti*-$B_{18}H_{22}$ is particularly more challenging given the more sophisticated cage structure compared to many other polyhedral boranes, rendering classical spectroscopic tools such as ^{11}B NMR less informative for routine structural characterization. These challenges are particularly pronounced when analyzing asymmetrically functionalized B_{18}-based compounds, which can display up to 18 unique broad, quadrupolar chemical shifts in the ^{11}B NMR spectrum.[4] As a result, single crystal X-ray diffraction is an extremely valuable tool necessary to confirm the molecular structure of these boron clusters and has consequently proven instrumental in the synthetic investigations of this boron cluster family.

Derivatives of *anti*-$B_{18}H_{22}$ reported so far[5] give insight into the reactivity of the cluster (Figure 1). There have been several studies reporting the synthesis of di- and poly-functionalized B_{18}-based clusters. Interestingly, despite the report on the first monofunctionalized $B_{18}H_{22}$ clusters dating as early as 1968,[5f] chemical routes allowing to selectively position a single functional group at a predetermined vertex in this species are still lacking. For example, while several halogenation methods have led to the synthesis and isolation of 7-I and 4-Br, the 4-I and 7-Cl have been

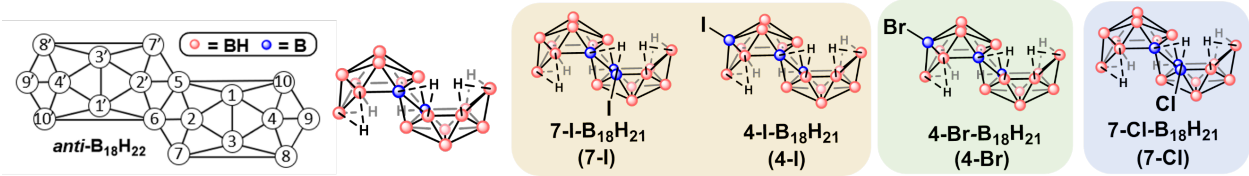

Figure 1. Structure and numbering scheme for *anti*-$B_{18}H_{22}$ and monohalogenated derivatives of *anti*-$B_{18}H_{22}$ in this and previously published works.[5a, 5c]

conspicuously missing. The synthesis of these compounds is important to decipher the effects of

simple substituents on the fluorescent properties of *anti*-$B_{18}H_{22}$.[6] Dramatic differences in luminescent properties have already been observed between compounds with similar structures; for example, while 7-I-*anti*-$B_{18}H_{21}$ exhibits phosphorescence at 525 nm and a quantum yield of 0.41,[5d] monobrominated 4-Br-*anti*-$B_{18}H_{21}$ possesses a dual emission property in which fluorescence at 410 nm and phosphorescence at 503 nm occur simultaneously.[5c] It remains unclear if these differences are attributable to substituent identity (I vs. Br), substituent location (B7 or B4), or a combination of both. To decouple the complex relationship between structure and luminescence, we expand the scope of monohalogenated B_{18} clusters with two new derivatives 4-I-*anti*-$B_{18}H_{21}$ (**4-I**) and 7-Cl-*anti*-$B_{18}H_{21}$ (**7-Cl**). Investigation of their luminescent properties revealed oxygen-insensitive phosphorescence in **4-I** and bright blue fluorescence in **7-Cl** that exhibits high efficiency with $\Phi = 0.80$.

2. Results and Discussion

2.1 Synthesis and Structural Analysis

2.1.1 Synthesis of 4-I-anti-$B_{18}H_{21}$ and 7-Cl-$B_{18}H_{21}$: A procedure used previously[5a] to prepare 4,4'-I_2-$B_{18}H_{20}$ was optimized to produce monohalogenated 4-I-anti-$B_{18}H_{21}$. Specifically, 1 eq. I_2 and 50 mol% $AlCl_3$ were reacted for 18 hours with *anti*-$B_{18}H_{22}$ dissolved in dichloromethane. *In situ* analysis of the resulting product mixture indicated the dominant presence of $B_{18}H_{21}I$ in the negative mode of electrospray ionization (ESI) mass spectrum (Figure S1). The pure monoiodinated compound was obtained in 43% isolated yield after purifying the crude product mixture by column chromatography on acidified silica gel. Spectroscopic characterization of purified product through ^{11}B NMR indicated an asymmetric boron cluster species with a diagnostic resonance corresponding to the newly substituted boron vertex at -49.2 ppm (Figures S2-4). Fifteen of the remaining peaks in the ^{11}B NMR spectrum show distinctive couplings to protons, overall confirming the monosubstitution pattern. Single crystal X-ray diffraction further confirmed the identity of the B4-substituted compound **4-I** (Figures 2, S15).

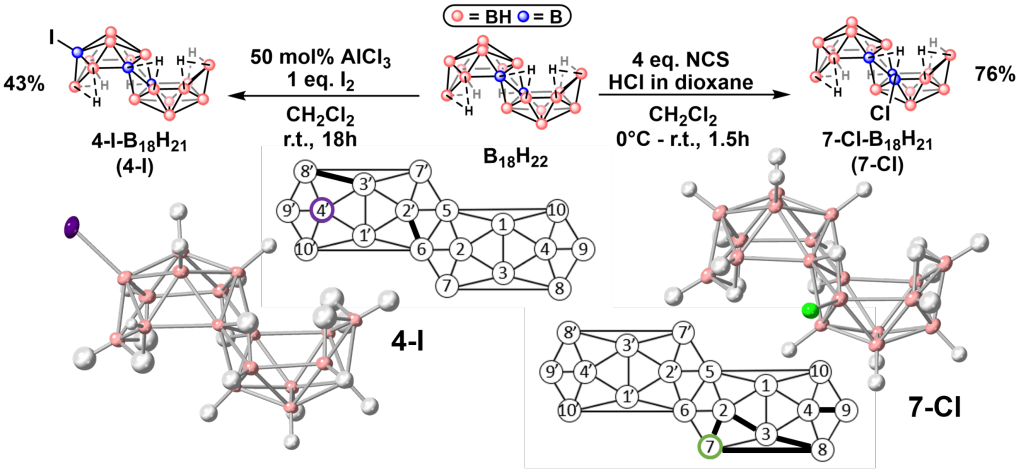

Figure 2. Synthetic schemes and crystal structures of **4-I** (left) and **7-Cl** (right), with significant bond lengthening denoted as bold bonds in the numbered structures. Thermal ellipsoids are drawn at 50% probability.

Success with the synthesis of **4-Br** previously and **4-I** in this study prompted us to expand this approach towards chlorination potentially targeting the B4 vertex through *in situ* generation of Cl_2 gas. This, however, proved challenging given the high reactivity of diatomic chlorine. When *anti*-$B_{18}H_{22}$ was treated with SO_2Cl_2 and $AlCl_3$ in 1,2-dichloroethane, the major species observed by electrospray ionization was $B_{18}H_{20}Cl_2$ (*m/z* = 284.24) accompanied by less intense mass peaks corresponding to $B_{18}H_{21}Cl$ and $B_{18}H_{19}Cl_3$. Purification by column chromatography on acidified silica gel produced the dichlorinated product, which appeared pure by mass spectrometry (Figure S9). However, analysis of this sample by ^{11}B NMR spectroscopy revealed two sets of boron resonances that indicated the sample contained two dichlorinated isomers (Figures S10-11). Neither modifications to this protocol nor the exploration of alternative electrophilic halogenation methods produced the desired B4-chlorinated products as a single isomer that could be successfully isolated chromatographically. Surprisingly, over the course of our studies, we discovered a set of conditions that produces a chlorinated isomer of $B_{18}H_{22}$ in which the B4 vertex remains unfunctionalized. Specifically, when the parent borane was reacted with Cl_2 gas produced *in situ* by treating N-chlorosuccinimide (NCS) with HCl/dioxane in dichloromethane[7] (Figure 2), the only mass observed in the mass spectrum of the crude reaction mixture corresponded to $B_{18}H_{21}Cl$ (*m/z* = 250.32). After purification by filtration and an aqueous workup, the pure sample was analyzed by ^{11}B NMR (Figures S5-8). The presence of more than 9 apparent boron resonances suggested an asymmetric cluster structure, and the newly substituted boron vertex was denoted by a singlet at -0.88 ppm. The significant difference between this chemical shift and the -49.2 ppm resonance observed in **4-I** led us to suspect that the chloride substituent could reside on a vertex other than B4. Subsequent analysis by single crystal X-ray diffraction revealed that this molecule was indeed the B7-functionalized product, 7-Cl-$B_{18}H_{21}$ (Figure S16). The apparent preference for B7 chlorination under the employed conditions was surprising given that the only other B7-substituted $B_{18}H_{22}$ derivative reported to date, **7-I**, forms from the reaction of *anti*-$B_{18}H_{22}$ with I_2 in ethanol. Similarities between the **7-Cl** and **7-I** reaction conditions, such as the absence of $AlCl_3$ catalyst, suggest that vertex preference could be dictated by the reacting intermediates (i.e., X_2 vs X^+) arising from the halogenation conditions. While $AlCl_3$ assists in the formation of X^+ to yield B4 functionalization, B7 products likely form from the reaction of the parent borane with X_2, which is assisted by diatomic bond polarization from the employed solvent.[8] As noted by previous work on the chlorination of carborane-based compounds, preferential site substitution (in this case, B7) could arise from a radical reaction favoring the kinetic product.[9] Notably, we attempted to synthesize the related 7-Br-*anti*-$B_{18}H_{21}$ cluster through similar means of employing N-bromosuccinimide activation. Indeed, we were able to purify a $B_{18}H_{21}Br$ compound (Figures S12-14) but have since been unable to confirm its location on the boron cage through single crystal X-ray diffraction due to our inability to grow X-ray quality crystals.

2.1.2 Structural Analysis of halogenated derivatives: Analysis of the monohalogenated $B_{18}H_{22}$ clusters through single crystal X-ray diffraction reveals that functionalization of the parent borane with halides leaves the overall cluster geometry intact (Table 1). Most bond lengths fit within three standard uncertainties compared to the parent $B_{18}H_{22}$, however the halogenated derivatives exhibit overall longer bonds. Select lengths of the newly synthesized compounds **4-I** and **7-Cl** are

Table 1. Select bond lengths (Å) of $B_{18}H_{22}$,[3] 4-I, 7-Cl, 7-I,[5a] and 4-Br[5c] with deviations from $B_{18}H_{22}$ greater than three standard uncertainties highlighted in blue. For 4-I, connectivities are B' and B6 instead of B5 (e.g., B1'-B6).

Connectivity	$B_{18}H_{22}$•C_6H_6	4-I•2C_6H_6	7-I	7-Cl•2C_6H_6	4-Br•2C_6H_6
B1-B2	1.786(5)	1.786(4)	1.780(5)	1.788(4)	1.750(7)
B1-B3	1.778(5)	1.786(5)	1.785(5)	1.782(4)	1.767(7)
B1-B4	1.786(5)	1.796(5)	1.806(5)	1.792(4)	1.804(6)
B1-B5 or B6	1.746(5)	1.754(4)	1.754(5)	1.757(4)	1.753(7)
B1-B10	1.74(5)	1.753(4)	1.754(5)	1.755(4)	1.766(7)
B2-B3	1.746(5)	1.766(4)	1.767(5)	1.769(4)	1.760(7)
B2-B5 or B6	1.765(5)	1.807(4)	1.800(5)	1.758(4)	1.816(7)
B2-B7	1.774(5)	1.792(5)	1.787(5)	1.799(4)	1.793(7)
B3-B4	1.774(5)	1.775(4)	1.780(5)	1.776(4)	1.772(7)
B3-B7	1.746(5)	1.756(4)	1.766(5)	1.758(4)	1.763(7)
B3-B8	1.723(5)	1.751(4)	1.761(5)	1.758(4)	1.758(7)
B4-B8	1.789(5)	1.801(4)	1.791(5)	1.802(4)	1.811(7)
B4-B9	1.702(5)	1.721(5)	1.712(5)	1.732(4)	1.735(7)
B4-B10	1.775(5)	1.781(4)	1.788(5)	1.785(4)	1.768(7)
B5 or B6-B10	1.968(5)	1.980(4)	1.971(5)	1.977(4)	1.990(7)
B5 or B6-B7	1.815(5)	1.820(5)	1.817(5)	1.823(4)	1.824(7)
B7-B8	1.946(5)	1.965(5)	1.972(5)	1.982(4)	1.973(7)
B8-B9	1.795(5)	1.797(5)	1.796(5)	1.790(4)	1.806(7)
B9-B10	1.783(5)	1.784(5)	1.778(5)	1.788(4)	1.789(7)
B-X	-	1.965(4)	2.173(5)	1.746(3)	1.906(7)

compared to those of $B_{18}H_{22}$ and the previously reported monohalogenated clusters **7-I** and **4-Br**. The most significant changes occur at bonds closest to the functionalized vertex. All structures exhibit a significant lengthening of B3-B8 and, except for **4-I**, B7-B8 bonds. Similarly, the B2-B5 (B2'-B6 for **4-I**) bonds show >0.035Å increases in every compound except **7-Cl**, in which it is slightly contracted. This contraction is compensated by significant lengthening in the B2-B3 and B2-B7 bonds of the chlorinated molecule. It is also worth noting that the B4-B9 connectivity is longer in all compounds, however **7-Cl** and **4-Br** show a remarkably longer B4-B9 bond than their iodinated analogues, **7-I** and **4-I**.

2.2 Photoluminescence Data

To gain insight into the effect of halogenation on the photophysical properties of B_{18}-based clusters, absorption and emission data of **4-I** and **7-Cl** were gathered in cyclohexane solution (Figure 3). The features in the absorption spectrum of **4-I** remain similar to the parent borane, but the absorptivity is diminished to $\varepsilon = 4400\ M^{-1}cm^{-1}$, which is close to the absorptivity of **7-I** (Table 2, Figure S17). Like **7-I**, **4-I** exhibits phosphorescence albeit at a slightly higher emission energy of 514 nm, with no evidence of the dual luminescence observed in **4-Br**. This can be attributed to the heavy atom effect, which lends spin-orbit coupling (SOC) to the molecule that permits intersystem crossing (ISC) from the excited singlet to triplet state. In this case, the increased size and weight of iodide compared to bromide results in greater SOC/ISC and therefore complete phosphorescence. These data suggest that the absorption coefficient, emission wavelength, and nature of the luminescent process (fluorescence vs. phosphorescence) are primarily dictated by the identity of the substituent rather than its location. However, the 50% reduction in quantum yield

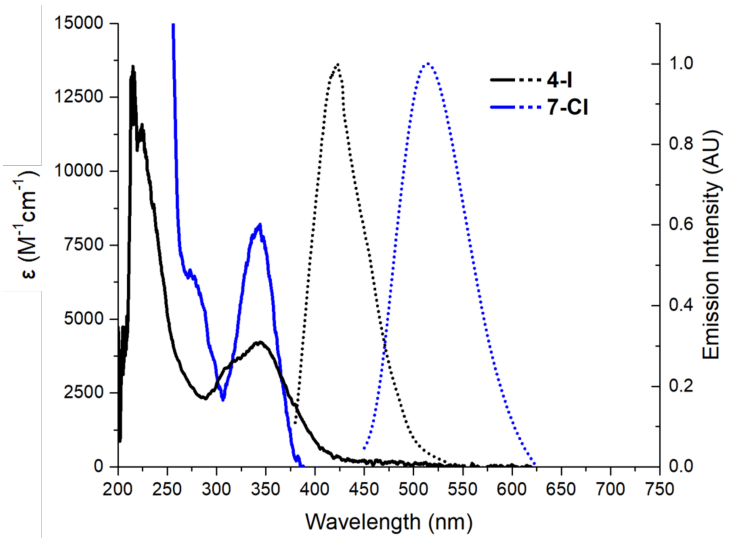

Figure 3. Absorption (solid) and emission (dotted) spectra of **4-I** and **7-Cl** in cyclohexane. λ_{exc} = 340 nm.

when iodide resides at B4 (Φ = 0.16) as opposed to B7 (Φ = 0.41) highlights the potentially inconspicuous effects of substituent location. Another interesting distinction between the emission features of the two iodinated clusters is oxygen sensitivity; phosphorescence, which originates from the triplet excited state, is typically subject to quenching by molecular oxygen. Consequently, the quantum yield of phosphorescent compounds improves under oxygen-free conditions. While this is observed with **7-I**, the quantum yield and lifetime of **4-I** remain unchanged upon degassing the cyclohexane solution (Figure S18). Typically, such insensitivity is caused by the inability of oxygen to interact with the molecule in the excited state due to either significant steric hindrance or obstruction of the oxygen reactive site.[10] **4-I** does not possess enough steric bulk to apply to the former, and quenching by oxygen has been observed in other B4-halogenated derivatives, which suggests that the latter is also unlikely. Rather, the insensitivity of phosphorescence to quenching by oxygen could be caused by the spatial distribution of valence orbitals in **4-I**. Specifically, the Natural Transition Orbitals (NTOs) determined from DFT calculations for the triplet excited state of **4-I** (Figure S21) show an electron NTO that is distributed across the entire boron cluster, whereas the hole NTO resides mainly localized on the iodide substituent. As phosphorescence quenching by oxygen takes place via triplet energy transfer using a Dexter mechanism, sufficient overlap is required between the valence orbitals of the interacting species (**4-I** and O_2).[11] Therefore, spatial confinement of the hole NTO in **4-I** could inhibit energy transfer by offering ineffective overlap with the corresponding molecular orbital on oxygen.

7-Cl also exhibited interesting absorption and emission properties (Figure S19). First, the absorptivity (ε = 8200 $M^{-1}cm^{-1}$) exceeds that of $B_{18}H_{22}$ and is on par with the absorptivity of the only other chlorinated compound reported to date.[5d] In contrast to the other halogenated compounds, **7-Cl** exhibits exclusively fluorescent emission at 418 nm. The absence of phosphorescence can be explained in part by the lighter and smaller nature of the chloride substituent compared to iodide or bromide. In addition, the difference in energy between the HOMO and HOMO-1 is large (ΔE = 0.9 eV). These orbitals have large contributions from orthogonal p-orbitals on the chloride atom and, following El-Sayed's rules,[11] are responsible for the change in angular momentum needed for effective SOC. The large energy separation between the filled valence orbitals results in poor SOC and raises the energy for the S_2 and T_2 states (HOMO-1 → LUMO, S_2 = 5.5 eV, T_2 = 5.1 eV), which further contributes to the inefficient ISC (Figure S22). While population of the excited triplet state does occur, phosphorescence is only visible as a shoulder at ~500 nm in the emission spectrum at 77 K (Figures S19-20). Therefore,

Table 2. Summary of photophysical data of monohalogenated $B_{18}H_{22}$ clusters in cyclohexane solution.[3,5a,c,e] [a]Measured in oxygen-free cyclohexane. λ_{exc} = 350 nm for quantum yield measurements of **4-I** and **7-Cl**. See Figures S11-13 for data.

Compound	λ_{abs} (nm)	ε ($M^{-1}cm^{-1}$)	λ_{em} (nm)	Φ	τ (μs)
$B_{18}H_{22}$	335	6800	408	0.97	0.0112
4-I-$B_{18}H_{21}$ (**4-I**)	342	4400	514	0.16[a]	1.2[a]
7-I-$B_{18}H_{21}$(**7-I**)	365	4900	525	0.41[a]	27[a]
7-Cl-$B_{18}H_{21}$ (**7-Cl**)	344	8200	418	0.80	0.0083
4-Br-$B_{18}H_{21}$ (**4-Br**)	341	1900	410, 503	0.07[a]	0.0103, 11.6[a]

the fluorescent nature of emission is maintained under ambient conditions and is red-shifted only slightly from the parent compound. The lifetime (8.3 ns) of this process is too fast to permit luminescence quenching by oxygen, and therefore does not change between ambient and degassed solutions. The quantum yield of **7-Cl** is also one of the highest of all B_{18}-based compounds reported to date, with Φ = 0.80.

3. Conclusion The syntheses of two new halogenated *anti*-$B_{18}H_{22}$ derivatives, 4-I-*anti*-$B_{18}H_{21}$ (**4-I**) and 7-Cl-*anti*-$B_{18}H_{21}$ (**7-Cl**) have been reported and benchmarked in the context of previously reported monohalogenated analogues. While electrophilic halogenation at the B4 vertex has successfully produced **4-Br** and **4-I**, attempts to synthesize the analogous chlorinated structure in this work instead resulted in **7-Cl**, which is the only reported B7-substituted $B_{18}H_{22}$ derivative apart from **7-I**. The structures of these compounds derived from single crystal X-ray diffraction show the overall cluster geometry is unperturbed, however significant bond lengthening between the B3-B8 and B7-B8 connectivities is observed for most clusters. In contrast to the other halogenated compounds, **7-Cl** exhibits B2-B5 bond contraction coupled with lengthening between the neighboring B2-B3 and B2-B7 bonds. While these minor structural differences exist, it is clear from the photophysical data that the absorption, emission, and quantum yields are greatly influenced by the identity and placement of halides. Interestingly, ε seems to be largely affected by the halide identity, with only **7-Cl** exhibiting improved absorptivity over the unfunctionalized borane. In contrast, the quantum yield is highly susceptible to all aspects of structural modification; significant differences are not only observed between different halides, but also in vertex-differentiated clusters containing the same halide. As research into the synthetic and photoluminescent properties of *anti*-$B_{18}H_{22}$ derivatives grows, structure-function relationships will become an increasingly important aspect of chromophore design. To that end, this work expands the foundation of synthetic modification of *anti*-$B_{18}H_{22}$, provides additional structural evidence through single crystal X-ray crystallography, and expands our understanding of the resulting luminescent properties of the substituted compounds.

Acknowledgements

A. M. S. acknowledges NSF Grants CHE-1846849 and DGE-1650604 (GRFP to K. P. A.). We thank Boron Specialties for the gift of $B_{18}H_{22}$. A. M. S. dedicates this work to Prof.

Arnie Rheingold for his immense contributions to the field and many fruitful collaborations over the past decade.

References

1. Recent representative examples: (a) K. K. Hollister, A. Molino, G. Breiner, J. E. Walley, K. E. Wentz, A. M. Conley, D. A. Dickie, D. J. D. Wilson and R. J. Gilliard, *J. Am. Chem. Soc.*, 2022, **144**, 590-598. (b) W. Yang, K. E. Krantz, L. A. Freeman, D. A. Dickie, A. Molino, A. Kaur, D. J. D. Wilson and R. J. Gilliard Jr, *Chem. Eur. J.*, 2019, **25**, 12512-12516. (c) X. Su, T. A. Bartholome, J. R. Tidwell, A. Pujol, S. Yruegas, J. J. Martinez and C. D. Martin, *Chem. Rev.*, 2021, **121**, 4147-4192. (d) K. O. Kirlikovali, J. C. Axtell, K. Anderson, P. I. Djurovich, A. L. Rheingold and A. M. Spokoyny, *Organometallics*, 2018, **37**, 3122-3131. (e) Z. Huang, S. Wang, R. D. Dewhurst, N. V. Ignat'ev, M. Finze and H. Braunschweig, *Angew. Chem. Int. Ed.*, 2020, **59**, 8800-8816. (f) Y. Lebedev, C. Apte, S. Cheng, C. Lavigne, A. Lough, A. Aspuru-Guzik, D. S. Seferos and A. K. Yudin, *J. Am. Chem. Soc*, 2020, **142**, 13544-13549. (g) H. S. Soor, D. B. Diaz, K. I. Burton and A. K. Yudin, *Angew. Chem. Int. Ed.*, 2021, **60**, 16366-16371. (h) X. Wu, J. Guo, Y. Quan, W. Jia, D. Jia, Y. Chen and Z. Xie, *J. Mater. Chem. C*, 2018, **6**, 4140-4149. (i) J. Wang, N. Wang, G. Wu, S. Wang and X. Li, *Angew. Chem. Int. Ed.*, 2019, **58**, 3082-3086. (j) K. Zhang, Y. Shen, X. Yang, J. Liu, T. Jiang, N. Finney, B. Spingler and S. Duttwyler, *Chem. Eur. J.*, 2019, **25**, 8754-8759. (k) Ž. Ban, Z. Karačić, S. Tomić, H. Amini, T. B. Marder and I. Piantanida, *Molecules*, 2021, **26**. (l) J. He, F. Rauch, A. Friedrich, J. Krebs, I. Krummenacher, R. Bertermann, J. Nitsch, H. Braunschweig, M. Finze and T. B. Marder, *Angew. Chem. Int. Ed.*, 2021, **60**, 4833-4840. (m) A. V. Marsh, M. J. Dyson, N. J. Cheetham, M. Bidwell, M. Little, A. J. P. White, C. N. Warriner, A. C. Swain, I. McCulloch, P. N. Stavrinou, S. C. J. Meskers and M. Heeney, *Adv. Electron. Mater.*, 2020, **6**, 2000312. (n) J. Ochi, K. Tanaka and Y. Chujo, *Angew. Chem. Int. Ed.*, 2020, **59**, 9841-9855. (o) L. Ji, S. Griesbeck and T. B. Marder, *Chem. Sci.*, 2017, **8**, 846-863. (p) J. C. Axtell, K. O. Kirlikovali, P. I. Djurovich, D. Jung, V. T. Nguyen, B. Munekiyo, A. T. Royappa, A. L. Rheingold and A. M. Spokoyny, *J. Am. Chem. Soc.*, 2016, **138**, 15758-15765. (q) K. O. Kirlikovali, J. C. Axtell, A. Gonzalez, A. C. Phung, S. I. Khan and A. M. Spokoyny, *Chem. Sci.*, 2016, **7**, 5132-5138. (r) P. Li, D. Shimoyama, N. Zhang, Y. Jia, G. Hu, C. Li, X. Yin, N. Wang, F. Jäkle and P. Chen, *Angew. Chem. Int. Ed.*, 2022, **61**, e202200612. (s) Z. Wu, J. Nitsch, J. Schuster, A. Friedrich, K. Edkins, M. Loebnitz, F. Dinkelbach, V. Stepanenko, F. Würther, C. M. Marian, L. Ji and T. B. Marder, *Angew. Chem. Int. Ed.*, 2020, **59**, 17137-17144. (t) T. Butler, M. Zhuang and C. L. Fraser, *J. Phys. Chem. C*, 2018, **122**, 19090-19099. (u) S. Ohtani, M. Gon, K. Tanaka and Y. Chujo, *Macromolecules*, 2019, **52**, 3387-3393. (v) J. Li, J. Xu, L. Yan, C. Lu and H. Yan, *Dalton Trans.*, 2021, **50**, 8029-8035. (w) K. L. Martin, J. N. Smith, E. R. Young and K. R. Carter, *Macromolecules*, 2019, **52**, 7951-7960. (x) S. Sinha, Z. Kelemen, E. Hümpfner, I. Ratera, J.-P. Malval, J. P. Jurado, C. Viñas, F. Teixidor and R. Núñez, *Chem. Commun.*, 2022, **58**, 4016-4019. (y) X. Wu, J. Guo, Y. Cao, J. Zhao, W. Jia, Y. Chen and D. Jia, *Chem. Sci.*, 2018, **9**, 5270-5277. (z) A. V. Marsh, N. J. Cheetham, M. Little, M. Dyson, A. J. P. White, P. Beavis, C. N. Warriner, A. C. Swain, P. N. Stavrinou and M. Heeney, *Angew. Chem. Int. Ed.*, 2018, **57**, 10640-10645. (aa) S. Kim, J. H. Lee, H. So, M. Kim, M. S. Mun, H. Hwang, M. H. Park and K. M. Lee, *Inorg. Chem. Front.*, 2020, **7**, 2949-2959.

2. J. Ševčík, P. Urbánek, B. Hanulíková, T. Čapková, M. Urbánek, J. Antoš, M. G. S. Londesborough, J. Bould, B. Ghasemi, L. Petřkovský and I. Kuřitka, *Materials*, 2021, **14**.

3. L. Cerdán, J. Braborec, I. Garcia-Moreno, A. Costela and M. G. S. Londesborough, *Nat. Commun.*, 2015, **6**, 5958.

4. M. G. S. Londesborough, J. Dolanský, T. Jelínek, J. D. Kennedy, I. Císařová, R. D. Kennedy, D. Roca-Sanjuán, A. Francés-Monerris, K. Lang and W. Clegg, *Dalton Trans.*, 2018, **47**, 1709-1725.

5. (a) M. G. S. Londesborough, J. Dolanský, J. Bould, J. Braborec, K. Kirakci, K. Lang, I. Císařová, P. Kubát, D. Roca-Sanjuán, A. Francés-Monerris, L. Slušná, E. Noskovičová and D. Lorenc, *Inorg. Chem.*, 2019, **58**,

10248-10259. (b) V. Saurí, J. M. Oliva, D. Hnyk, J. Bould, J. Braborec, M. Merchán, P. Kubát, I. Císařová, K. Lang and M. G. S. Londesborough, *Inorg. Chem.*, 2013, **52**, 9266-9274. (c) K. P. Anderson, M. A. Waddington, G. J. Balaich, J. M. Stauber, N. A. Bernier, J. R. Caram, P. I. Djurovich and A. M. Spokoyny, *Dalton Trans.*, 2020, **49**, 16245-16251. (d) M. G. S. Londesborough, K. Lang, W. Clegg, P. G. Waddell and J. Bould, *Inorg. Chem.*, 2020, **59**, 2651-2654. (e) K. P. Anderson, A. S. Hua, J. B. Plumley, A. D. Ready, A. L. Rheingold, T. L. Peng, P. I. Djurovich, C. Kerestes, N. A. Snyder, A. Andrews, J. R. Caram, A. M. Spokoyny, preprint DOI: 10.26434/chemrxiv-2022-h70dk. (f) F. P. Olsen, R. C. Vasavada, M. F. Hawthorne. *J. Am. Chem. Soc.*, 1968, **90**, 3946-3951.

6. (a) M. G. S. Londesborough, D. Hnyk, J. Bould, L. Serrano-Andrés, V. Sauri, J. M. Oliva, P. Kubát, T. Polívka and K. Lang, *Inorg. Chem.*, 2012, **51**, 1471-1479. (b) M. G. S. Londesborough, J. Dolanský, L. Cerdán, K. Lang, T. Jelínek, J. M. Oliva, D. Hnyk, D. Roca-Sanjuán, A. Francés-Monerris, J. Martinčík, M. Nikl and J. D. Kennedy, *Adv. Opt. Mater.*, 2017, **5**, 1600694. (c) L. Cerdán, A. Francés-Monerris, D. Roca-Sanjuán, J. Bould, J. Dolanský, M. Fuciman and M. G. S. Londesborough, *J. Mater. Chem. C*, 2020, **8**, 12806-12818.

7. Synthesis derived from: A. Nishiguchi, K. Maeda and S. Miki, *Synthesis*, 2006, 4131.

8. (a) W. Lorpaiboon and P. Bovonsombat, *Org. Biomol. Chem.*, 2021, **19**, 7518-7534. (b) M. Zhang and C. R. F. Lund, *J. Phys. Chem. A*, 2002, **106**, 10294-10301. (c) G. L. Borosky, S. Stavber and K. K. Laali, *Top. Catal.*, 2018, **61**, 636-642.

9. (a) P. Farràs, C. Viñas, R. Sillanpää, F. Teixidor and M. Rey, *Dalton Trans.*, 2010, **39**, 7684-7691. (b) P. Farràs, C. Viñas and F. Teixidor, *J. Organomet. Chem.* 2013, **747**, 119-125.

10. (a) L. Straub, D. González-Abradelo and C. A. Strassert, *Chem. Comm.*, 2017, **53**, 11806-11809. (b) T. Zhang, C. Wang and X. Ma, *Ind. Eng. Chem. Res.*, 2019, **58**, 7778-7785. (c) I. O. Koshevoy, Y.-C. Lin, Y.-C. Chen, A. J. Karttunen, M. Haukka, P.-T. Chou, S. P. Tunik and T. A. Pakkanen, *Chem. Comm.*, 2010, **46**, 1440-1442.

11. (a) G. L. Closs, P. Piotrowiak, J. M. MacInnis, G. R. Fleming, *J. Am. Chem. Soc.*, 1988, **110**, 2643-2655. (b) G. L. Closs, M. D. Johnson, J. R. Miller, P. Piotrowiak, *J. Am. Chem. Soc.*, 1989, **111**, 3751-3753. (c) S. K. Lower and M. A. El-Sayed, *Chem. Rev.*, 1966, **66**, 199-241.